SimBuild
2024

Eleventh National Conference of IBPSA-USA
Denver, Colorado
May 21 – 23, 2024

Unveiling the Role of Deployment in the Performance of ASHRAE Guideline 36

Sen Huang, Yeobeom Yoon, Piljae Im, Helia Zandi, and Jamie Lian
Oak Ridge National Laboratory, Oak Ridge, TN

Abstract

This paper presents a simulation-based assessment of how the deployment of ASHRAE Guideline 36: High-Performance Sequences of Operation for HVAC (*G36*) impacts the energy performance of G36. In this assessment, an EnergyPlus model and a control sequence in G36 are co-simulated. This EnergyPlus model represents a variable air volume system that serves Oak Ridge National Laboratory's Flexible Research Platform 2 Building. When performing the assessment, we consider six cases, to represent various deployments. In Case 1 and 2, ideal and poor local control loops (*LCLs*) are considered, respectively. In Case 3 and 4, ideal LCLs with positive and negative sensor bias are considered, respectively. In Case 5 and 6, poor LCLs with positive and negative sensor bias are considered, respectively. Those assessment results suggest 1 $^{\circ}C$ sensor bias leads to 2.5 time changes in the energy savings from G36. They also reveal that the control performance of LCL results in 2.3 time differences in the peak power.

Introduction

To accelerate real-world adoption, there have been longstanding interests in assessing ASHRAE Guideline 36: High-Performance Sequences of Operation for Heating, Ventilation, and Air Conditioning (HVAC) Systems (*G36*) (ASHRAE 2018) with simulation (Faulkner et al. 2023). Although providing critical insights, existing efforts in this regard don't consider the impact of the deployment of G36. In this context, the deployment of G36 refers to establishing a software/hardware mechanism that samples measurements from the controlled HVAC system and actuates the control actions that are generated by supervisor control sequences (SCSs) in G36. The deployment of SCSs, including the ones in G36, can vary by many factors, including the hardware condition (e.g., good or faulty) and the technician's skill levels. The diversity of the G36 deployment gives rise to issues such as sensor errors and poor local control loops (*LCLs*) (Zhang et al. 2021). However, this diversity was not well captured by the existing efforts, as elaborated in the *Literature Review* Section.

This paper presents a simulation-based assessment of G36 by considering the diversity of the G36 deployment. In this assessment, an EnergyPlus (Crawley et al. 2001) model and a control sequence in G36 are co-simulated. This EnergyPlus model represents a variable air volume (VAV) system that serves Oak Ridge National Laboratory's Flexible Research Platform 2 (FRP-2) Building. The control sequence, i.e., the supply air temperature reset control (*SAT_Reset*), resets the discharge air temperature setpoint of the VAV system based on the measurements, such as outdoor temperature and the zone temperature. When performing the assessment, we designed six simulation cases, as summarized below, to represent various deployment processes. In Case 1 and 2, ideal and poor LCLs are considered, respectively. In Case 3 and 4, ideal LCLs with positive and negative sensor bias are considered, respectively. In Case 5 and 6, poor LCLs with positive and negative sensor bias are considered, respectively.

The rest of the paper is organized as follows. We first summarize the existing studies in the literature and highlight the research gaps. We then describe the implementation of G36, LCLs, and sensor bias; as well as co-simulation settings. After that, we present the major results of the control assessment and the relevant discussions. At last, we conclude this paper and envision future work.

Literature Review

The existing studies on the simulation-based assessment of G36 can be categorized in two groups, depending on how G36 was implemented. In the first group (*Group 1*), G36 is implemented as part of the building energy models. For example, (Pang et al. 2020) integrated the occupant-centric building control sequences from G36 to the U.S. DOE Prototype Models, via the Energy Management System (EMS) module (U.S. Department of Energy 2018), to perform a nation-wide assessment of energy saving potential from those sequences. (Zhang et al. 2020) implemented both G36 and the studied VAV system using the Modelica Buildings library (Wetter et al. 2014) to assess its energy performance. In the second group (*Group 2*), G36 is co-simulated with building energy models. For instance, (Lee et al. 2022) implemented the SAT_Reset in Python (Van Rossum and Drake 2009) and co-simulated it with the U.S. DOE Prototype Models (Deru et al. 2011) to study how the energy performance of the SAT_Reset varies based on climate location. (Faulkner et al. 2023) implemented the G36 control sequences for both water-side and air-side equipment in Python and then co-simulated the resulting Python scripts with a simulated VAV system by the Modelica Buildings library.

Regardless of how G36 is implemented, the existing studies approximate the deployment of G36 with various assumptions for simplification. For example, the studies in Group 1 effectively assume the sampling of measurements is synchronized with the simulation step. Note that some assumptions may restrict the assessment of G36 to consider different types of deployment. For example, most of the existing studies assume the sampling of measurement is error-free, which prevents the deployment with faulty conditions from being considered. In addition, in the assessment performed by (Lee et al. 2022), the LCLs for controlling the zone temperature are implemented as ideal control loops, i.e. no overshooting or oscillations. In such a case, poor LCLs are excluded from the assessment.

Note that the limitations associated with those assumptions have been recognized in the literature. Some researchers studied how the error-free sensors affect the performance of G36. For example, (Li et al. 2023) studied the energy performance of two control sequences in G36 under the impact of various sensor faults. Nevertheless, systematical assessment of how the deployment affects the operation of G36 is seldom reported in the literature.

Methodology

This section details how the deployment is considered in the simulation-based assessment of G36. It starts with a brief introduction of the studied system; It then elaborates different deployments of G36 to the studied system; Finally, it discusses how those deployments are implemented in the co-simulation.

Studied System

As illustrated in Figure 1, the studied VAV system comprises one air handling unit (*AHU*), ten terminals, and one duct network. The AHU is composed of one direct expansion (*DX*) cooling coil, one DX heating coil, and one variable speed fan. Each terminal consists of one damper and one electric reheat coil. This VAV system is controlled by three LCLs:

- LCL #1 adjusts the speed of the fan to maintain the static pressure in the duct network at the setpoint.
- LCL #2 turns on/off the two-speed compressor to maintain the discharge air temperature at the setpoint.
- LCL #3 changes the position of the damper and the output of the reheat coil to maintain the zone temperature at the setpoint.

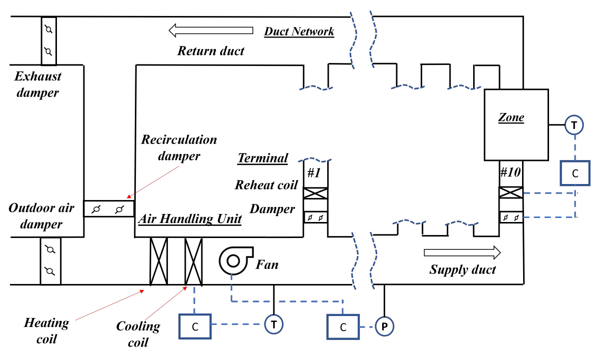

Figure 1: Studied VAV System

G36 Deployments

In this study, we deploy the SAT_Reset to the studied VAV system. This SAT_Reset resetting the setpoint of LCL #2 (*DATset*) with a trim & respond logic (Faulkner et al. 2023), based on zone temperatures and the outdoor temperature. Specifically, we keep increasing *DATset* until the thermal discomfort level exceeds a certain threshold or the *DATset* reaches the maximum value. The thermal discomfort level is characterized by the zone temperatures while the maximum value of *DATset* is determined by the outdoor temperature. When the thermal discomfort level exceeds a certain threshold, we keep decreasing *DATset* until the thermal discomfort level is lower than the threshold or the *DATset* reaches the minimum value. Likewise, when the *DATset* reaches the maximum value, *DATset* is set to be the maximum value. The deployment of the SAT_Reset includes

- setting up sensors to predictably sample the zone temperatures and the outdoor temperature.
- implementing the LCLs to adjust the operation status of devices in this VAV system based on the setpoint generated by the SAT_Reset.

Depending on the conditions of sensors and how LCLs are implemented, there is an infinite amount of deployments. Among those deployments, we select six representatives where three conditions for zone temperature sensors and two implementations of LCL #3 are considered, as summarized in Table 1. Those six cases couldn't represent all the possible G36 deployments. Instead, they are designed to represent extreme scenarios when deploying G36 and their results can help to identify the possible ranges by which the deployment can affect the energy performance of G36. In all studied deployments, the outdoor temperature sensor is error-free and LCL #1 and #2 are ideal, for simplicity's sake.

Table 1: Deployments of G36

Case	Zone Temperature Sensor (All Zones)	Local Control Loop #3
1	Error-free	Ideal
2	Error-free	Poor
3	1 $°C$ Bias	Ideal
4	-1 $°C$ Bias	Ideal
5	1 $°C$ Bias	Poor
6	-1 $°C$ Bias	Poor

Both the ideal and the poor version of LCL #3 are based on a Dual-Max control logic. Specifically, the former is implemented as a part of the building model. On the other hand, the latter employs an algorithm defined in Figure 2. Note that the poor version of LCL #3 uses the commonly available measurements and generally accessible actuation points. Both the ideal and the poor version of LCL #3 are synchronized with the simulation step.

Model Development & Implementation

We employ EnergyPlus to model the devices in the studied VAV system, LCL #1/#2, and the building envelope. The resulting EnergyPlus model is calibrated with real measurements from the FRP-2 Building (Im et al. 2020). In addition, we model the faulty sensors with the EnergyPlus objects called *FaultModel:ThermostatOffset*. Likewise, we represent the ideal version of LCL #3 with an EnergyPlus object *AirTerminal:SingleDuct:VAV:Reheat*.

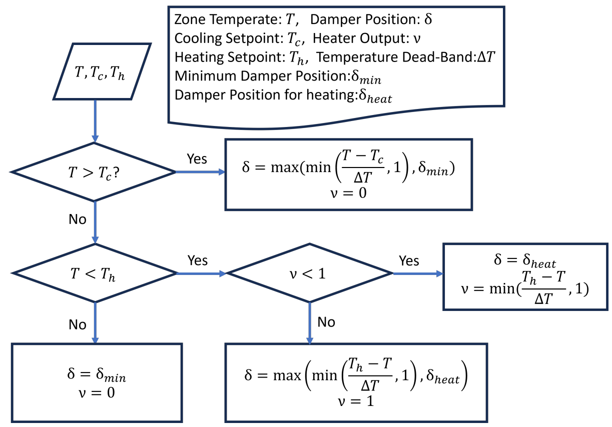

Figure 2: A control algorithm for Local Control Loop #3

The SAT_Reset and the control algorithm of LCL #3 in Figure 2 are implemented in Python and detailed descriptions can be found in (Faulkner et al. 2023).

We co-simulate EnergyPlus and Python via the The Building Controls Virtual Test Bed (Wetter, Haves, and Coffey 2008). The variables exchanged in the co-simulation, however, vary by the studied cases. As illustrated in Figure 3, in all cases, EnergyPlus sends the outdoor temperature to Python. In Case 1 and 2, EnergyPlus sends the zone temperature to Python. In the rest cases, EnergyPlus sends the faulty zone temperature to Python instead. In all cases, EnergyPlus receives DATset from Python. In Case 2, 5, and 6, EnergyPlus receives the terminal damper positions, and the reheat coil outputs, beside the DATset. The terminal damper positions are used to determine the actual flow rate of each terminal in EnergyPlus via an EnergyPlus object *EnergyManagementSystem:Actuator*.

Results & Discussions

We perform year-long simulations to assess the six cases. Detailed settings of those simulations are summarized in Table 2. Note that the energy consumption savings and the peak power reductions are calculated by comparing the results of all the studied cases to those of a case which is identical to Case 1 except the DATset is fixed at 12.8 $°C$.

As illustrated in Figure 4 are the annual energy consumption savings and the peak power reductions of all the studied cases. One can see that for all the cases, the SAT_Reset significantly reduces the energy consumption of the reheat coils and the cool coil. The effects in the en-

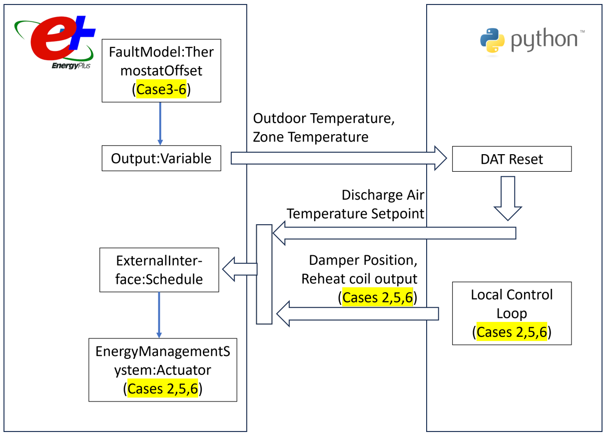

Figure 3: Co-simulation between EnergyPlus and Python

Table 2: Simulation Settings

Setting	**Description**
Weather	TMY3 data Knoxville, TN
Simulation Interval	1 minute
Co-simulation Interval	1 minute
Interval of the SAT_Reset	2 minute
Maximum Outdoor temperature for SAT Reset	21.1 $^{\circ}C$
Minimum Outdoor temperature for SAT Reset	15.6 $^{\circ}C$
Number of the ignored request in SAT Reset	2
Maximum value of DATset	18.3 $^{\circ}C$
Minimum value of DATset	12.8 $^{\circ}C$
Trim	0.1 $^{\circ}C$
Response	0.2 $^{\circ}C$
Maxium Response	0.6 $^{\circ}C$
DeadBand in the LCL #3	1 $^{\circ}C$
Cooling setpoint	22 $^{\circ}C$
Heating setpoint	20 $^{\circ}C$

ergy consumption of the fan are negligible. The results in Figure 4 also reveal that the deployment poses dramatic impacts on the energy performance of the SAT_Reset. The annual energy savings of the studied cases vary from 14% to 36% while the reduction in the peak power changes from -75% to 25%. A positive sensor bias leads to a lower total energy consumption and a higher peak electricity load. On the other hand, the peak power is also impacted by the implementation of LCL #3. With a poor control performance of LCL #3, the peak power increases while the ideal version of LCL #3 reduces the peak power.

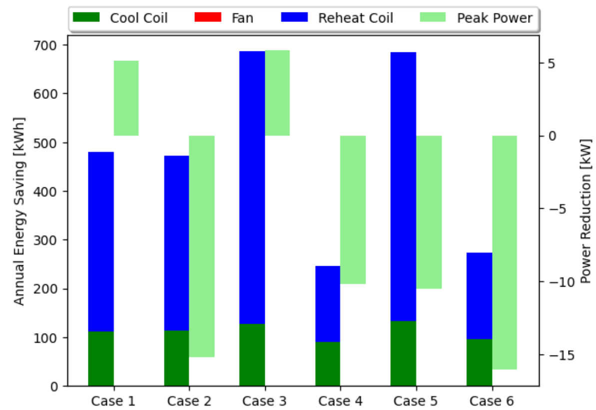

Figure 4: Annual energy consumption and the peak electricity load

To understand how different energy savings are achieved, we study the zone temperature in the studied cases. As shown in Figure 5, the zone temperatures in Case 3 and 5 are closer and much lower than those in other cases. This is because Case 3 and 5 include a positive sensor bias, which makes the VAV system overestimate the cooling load and thus over-cools the zones, resulting in a lower energy consumption of reheat coils. Likewise, the negative sensor bias in Case 4 and 6 leads to over-heated zones, resulting in the increased energy consumption of reheat coils. In addition, we also find the distribution of zone temperature is more skewed under the ideal version of LCL #3. Taking Case 1 as an example, zone temperatures in this case are maintained at 20 $^{\circ}C$, which is the heating setpoint. Note that the FRP-2 building is unoccupied and the VAV system is oversized. Therefore, the heating condition is the dominating operating condition of this building. On the other hand, zone temperatures in Case 2 change from 20 $^{\circ}C$ to 21 $^{\circ}C$ during most of the time.

Figure 6 illustrates the distribution of the discharge air temperature and the DATset. For all cases, the distribution of the DATset is almost identical. However, the actual value of the discharge air temperature varies by case, due to the different distributions of zone temperatures. Note that the studied VAV system is operated with a minimum outdoor air flow rate and the zone tempera-

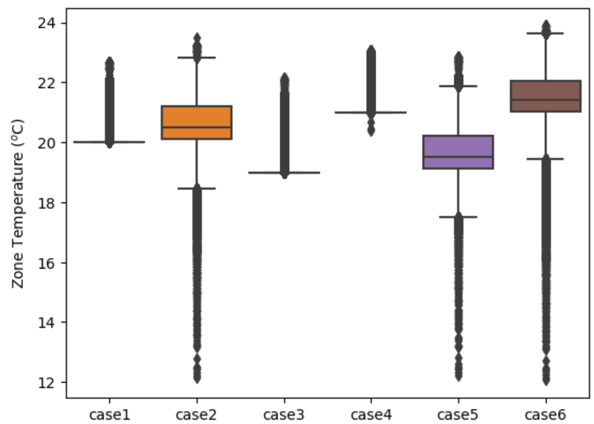

Figure 5: Distribution of the zone temperature

tures significantly impact the mixed air temperature.

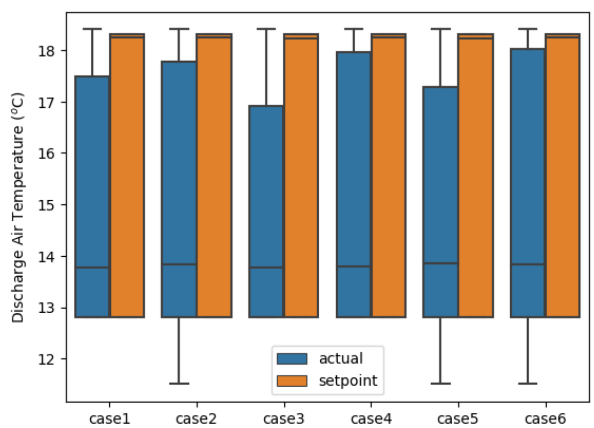

Figure 6: Distribution of the discharge air temperature

Figure 7 demonstrates zone temperature trajectory in Case 1 and 2 under a typical cooling day (July 7). We can see that in Case 1, the objectives for controlling the zone temperature are perfectly achieved. The zone temperatures are either equal to the heating/cooling setpoint or within the deadband. In addition, the zone temperature changes smoothly and there are no oscillations. On the other hand, in Case 2, the control performance is much worse. There are quite a few times when the zone temperatures are beyond the comfort deadband. There are also a large amount of oscillations in the zone temperature trajectories.

Figure 8 compares the electricity loads during the same cooling day in Case 1 and 2. As mentioned above, the FRP-2 building is unoccupied and it has a significant heating load during the night time even in summer. In Case 1, due to the heating demand, the electricity load is higher during the night time and the peak value occurs in the early morning. In Case 2, the general trend of the electricity load is similar to that in Case 1. However, the electricity load in Case 2 fluctuates dramatically due to the iterations in the LCLs #3, doubling the peak electricity load.

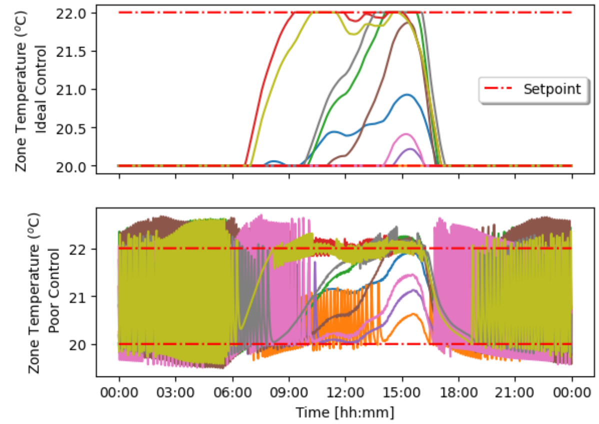

Figure 7: Zone temperature trajectory in Case 1 and 2

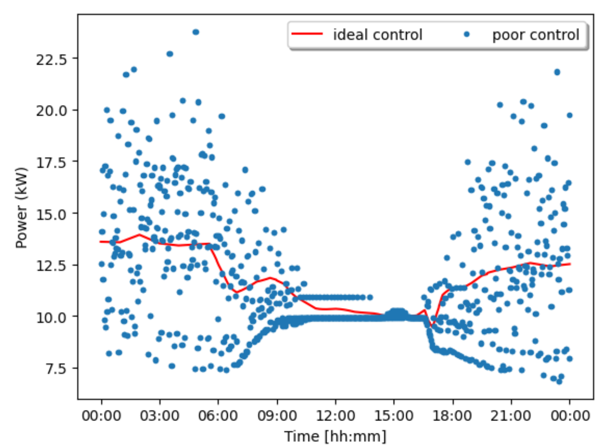

Figure 8: Total electricity load in Case 1 and 2

Conclusion

This paper quantitatively assesses how the deployment of G36 affects its control performance, based on a co-simulation between EnergyPlus and Python. Based on the assessment, we find that

- Energy savings from G36 is mainly due to the reduction of heating power.
- 1 $^{\circ}C$ sensor bias leads to 2.5-time changes in the energy savings from G36.
- The control performance of LCL #3 results in 2.3-time differences in the peak power.

These findings clearly emphasize the critical role of the deployment in determining the control performance of G36. Therefore, it is important to examine the deployment of G36, in terms of sensors and LCLs. The closer the deployment to the ideal situation, it is more likely to fully unleash the potential of G36 to improve the operation of building systems. Alternatively, researchers can consider incorporating the deployment in the ongoing enhancement of G36 to 1) provide more detailed guidance on how to adjust G36 based on a specific deployment and 2) develop smart control sequences that can adapt to a given deployment.

Due to the constraints of EnergyPlus, there are some limitations in this study. First, we have to exclude LCL #1 and #2 from the scope as EnergyPlus doesn't explicitly model the pressure distribution across the duct and doesn't allow it to overwrite the control of coils. Second, the minimum simulation interval in EnergyPlus is 1 minute, which is a little large to capture the short-term dynamics in the building operation. The short-term dynamics are critical when examining the control performance of G36. For example, when assessing the iterations of control sequences in LCL #3, measurements with second-level resolutions are required to avoid artificial oscillations. Thus, the results related to the peak power may be interpreted qualitatively rather than quantitatively.

Those limitations can be potentially resolved in the future study by adapting the new developments in building energy modeling. For example, one can replace the EnergyPlus model with a Spawn-of-energyplus model (Wetter et al. 2023). By doing so, one can faithfully represent the pressure drop in the duct and conduct a fine-time-resolution dynamic simulation.

Moreover, only one climate zone is considered in this study as we only have one calibrated model. However, understanding the qualitative and quantified conclusions varies by other zones with different heating and cooling loads requires including other climate zones in the simulation. This should be considered in future when more calibrated models are available.

Acknowledgment

This manuscript has been authored by UT-Battelle, LLC, under contract DE-AC05-00OR22725 with the US Department of Energy (DOE). The US government retains and the publisher, by accepting the article for publication, acknowledges that the US government retains a nonexclusive, paid-up, irrevocable, worldwide license to publish or reproduce the published form of this manuscript, or allow others to do so, for US government purposes. DOE will provide public access to these results of federally sponsored research in accordance with the DOE Public Access Plan (https://www.energy.gov/doe-public-access-plan).

References

ASHRAE. 2018. "Guideline 36-2018: High Performance Sequences of Operation for HVAC Systems."

Crawley, Drury B, Linda K Lawrie, Frederick C Winkelmann, Walter F Buhl, Y Joe Huang, Curtis O Pedersen, Richard K Strand, Richard J Liesen, Daniel E Fisher, Michael J Witte, et al. 2001. "EnergyPlus: creating a new-generation building energy simulation program." *Energy and buildings* 33 (4): 319–331.

Deru, Michael, Kristin Field, Daniel Studer, Kyle Benne, Brent Griffith, Paul Torcellini, Bing Liu, Mark Halverson, Dave Winiarski, Michael Rosenberg, et al. 2011. "US Department of Energy commercial reference building models of the national building stock."

Faulkner, Cary A, Robert Lutes, Sen Huang, Wangda Zuo, and Draguna Vrabie. 2023. "Simulation-based assessment of ASHRAE Guideline 36, considering energy performance, indoor air quality, and control stability." *Building and Environment* 240:110371.

Im, Piljae, Jaewan Joe, Yeonjin Bae, and Joshua R New. 2020. "Empirical validation of building energy modeling for multi-zones commercial buildings in cooling season." *Applied Energy* 261:114374.

Lee, Joon-Yong, Aowabin Rahman, Sen Huang, Amanda D Smith, and Srinivas Katipamula. 2022. "On-policy learning-based deep reinforcement learning assessment for building control efficiency and stability." *Science and Technology for the Built Environment* 28 (9): 1150–1165.

Li, Yanfei, Piljae Im, Seungjae Lee, Yeonjin Bae, Yeobeom Yoon, and Sangkeun Lee. 2023. "Sensor

Incipient Fault Impacts on Building Energy Performance: A Case Study on a Multi-Zone Commercial Building." *Buildings* 13 (2): 520.

Pang, Zhihong, Yan Chen, Jian Zhang, Zheng O'Neill, Hwakong Cheng, and Bing Dong. 2020. "Nationwide HVAC energy-saving potential quantification for office buildings with occupant-centric controls in various climates." *Applied Energy* 279:115727.

U.S. Department of Energy. 2018. "Application Guide for EMS."

Van Rossum, Guido, and Fred L Drake. 2009. *Python 3 reference manual*. CreateSpace.

Wetter, Michael, Kyle Benne, Hubertus Tummescheit, and Christian Winther. 2023. "Spawn: coupling Modelica Buildings Library and EnergyPlus to enable new energy system and control applications." *Journal of Building Performance Simulation*, pp. 1–19.

Wetter, Michael, Philip Haves, and Brian Coffey. 2008. "Building controls virtual test bed." Technical Report, Lawrence Berkeley National Lab.(LBNL), Berkeley, CA (United States).

Wetter, Michael, Wangda Zuo, Thierry S Nouidui, and Xiufeng Pang. 2014. "Modelica buildings library." *Journal of Building Performance Simulation* 7 (4): 253–270.

Zhang, Kun, David H Blum, Milica Grahovac, Jianjun Hu, Jessica Granderson, and Michael Wetter. 2020. "Development and Verification of Control Sequences for Single-Zone Variable Air Volume System Based on ASHRAE Guideline 36." Technical Report, Lawrence Berkeley National Lab.(LBNL), Berkeley, CA (United States).

Zhang, Liang, Matt Leach, Yeonjin Bae, Borui Cui, Saptarshi Bhattacharya, Seungjae Lee, Piljae Im, Veronica Adetola, Draguna Vrabie, and Teja Kuruganti. 2021. "Sensor impact evaluation and verification for fault detection and diagnostics in building energy systems: A review." *Advances in Applied Energy* 3:100055.